ELSEVIER

Journal of Power Sources 112 (2002) 184–190

JOURNAL OF POWER SOURCES

www.elsevier.com/locate/jpowsour

Characterization of a silver-ion conducting solid-state battery with a new compact battery discharge unit

R. Murugaraj[a], G. Govindaraj[a,*], S. Ramasamy[b]

[a]*Raman School of Physics, Pondicherry University, R.V. Nagar, Pondicherry 605014, India*
[b]*USIC, Pondicherry University, R.V. Nagar, Pondicherry 605014, India*

Received 29 April 2002; accepted 16 June 2002

Abstract

The polarization and discharge characteristics of solid-state batteries are examined by means of a conventional load resistor technique with high-performance mV or μA meters. In the present paper, to overcome the need for high-performance meters, a compact discharge–polarization unit is constructed. The new discharge unit does not require any other high input impedance accessories like, mV or μA meters. It is used to study the polarization and discharge characteristics of silver-ion conducting electrolytes such as: (a) the polycrystalline system: $((CH_3)_4N)_2Ag_{13}I_{15}$; (b) the silver boro-vanadate glassy system: $AgI–Ag_2O–B_2O_3–V_2O_5$; (c) the silver boro-molybdate glassy system: $AgI–Ag_2O–B_2O_3–MoO_3$. Solid-state batteries are fabricated with different cathode materials at various compositions and battery performance is studied with the new battery discharge unit.

Keywords: Silver-ion conductors; Battery discharge unit; Solid-state batteries; Polarization; Discharge characteristics

1. Introduction

In recent years, various crystalline and polycrystalline materials, glasses, composites and polymers have been synthesized for application in solid-state batteries [1–13]. Glassy and amorphous phases have gained more importance due to their high ionic conductivity and very low electronic conductivity. Among the fast ion conducting glasses, silver-ion conducting glasses were the first solid electrolytes to be used in solid-state electro-chemical devices for low specific energy applications. Nevertheless, research activities in this field are continuing because of the good stability of the material and the possibility of micro-battery applications [14–20]. In the present work, a new, laboratory-scale, discharge unit is constructed and used to study the performance of solid-state batteries fabricated with the silver-ion conducting solid electrolytes: $((CH_3)_4N)_2Ag_{13}I_{15}$ (SITMAI); 60% $AgI + 26.67\%$ $Ag_2O + 13.33\%$ (F_1 $B_2O_3 + F_2$ V_2O_5), termed SSBV; 60% $AgI + 26.67\%$ $Ag_2O + 13.33\%$ (F_1 $B_2O_3 + F_2$ MoO_3), termed SSBM. The polarization and discharge characteristics are studied with different compositions of the cathode mixture using the above discharge unit. The performance of the batteries and their results are reported.

2. Construction of new discharge unit

The circuit diagram for the new discharge unit is given in Fig. 1. The magnitude and specifications of the components are listed in Table 1. The circuit design is as follows. The integrated circuit band gap reference LM 336-2.5 (D3) is used to generate a stable reference voltage of 2.5 V. It is buffered by U1/4 so that the loading does not affect the reference source. The potential divider network R1–R2 is used to adjust and set a voltage which corresponds to the desired constant current. The values are chosen so that 1 V set by R2 corresponds to 1.000 mA or 100.0 μA full-scale of current drawn from the battery. U1/1 is used to control the current drawn from the battery. The operation amplifiers large open loop gain ensures that the voltage drop across the resistor R6 (1 kΩ for 1 mA or 10 kΩ for 100 μA range) caused by the current drawn from battery to be equal to the voltage set by R2. Thus, a constant current is drawn from the battery, irrespective of the battery terminal voltage. Diode D1 is used to protect the test battery against any charging current in the event of any problems/failure. The voltage drop across the standard resistor R5 is measured with a digital voltmeter (DVM) to ascertain the value of the discharge current. Alter-

* Corresponding author. Tel.: +91-413-655-991/735; fax: +91-413-655-265/255.
E-mail addresses: purm72@mailcity.com, ggraj_54@mailcity.com (G. Govindaraj).

0378-7753/02/$ – see front matter
PII: S0378-7753(02)00355-5

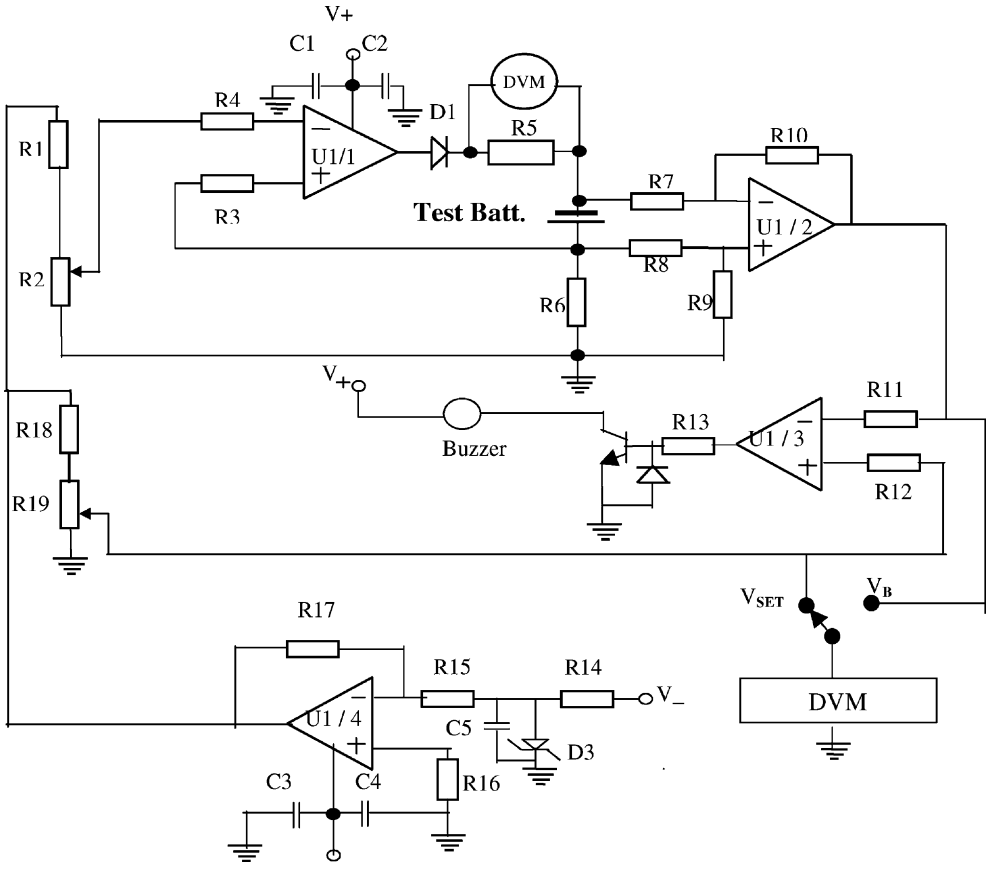

Fig. 1. Circuit diagram of battery discharge unit. Details of components are given in Table 1.

natively, a suitable analog mA/μA meter can also be used in place of R5, if analog indication is preferred.

A differential amplifier circuit using U1/2 is employed for monitoring the terminal voltage of the test battery during the discharge period. The potential divider network R18–R19 sets the desired limit of the terminal voltage up to which the battery can be discharged. The voltage can be set by closing the DVM switch to 'set' mode. When the switch is closed on 'measure' mode, it measures the terminal voltage of the test battery. U1/3 used as a voltage comparator compares the battery terminal voltage with the limit value set by R19. When the battery discharges and its terminal voltage falls below the set value, the output of U1/3 goes to positive saturation and activates a buzzer to provide an audible alarm to alert the user to record the parameters.

A set of 9 V flat-pack batteries, the output of which is regulated by standard three-pin regulators to +5 and −5 V, is used to power the circuit. DPM units, 3.5 digit LCD type (200 mV/2 V FS) driven by independent batteries, can be used so that the whole system can function independently of mains power. An optional unit, controlled by the output of U1/3, turns on a quartz clock when the measurement is started and turns off when the set level is reached. At that time, the audible alarm is raised. Setting the clock at 12.00 h at the start of the measurement helps to determine the time taken for the discharge. The unit through its relay contacts helps to connect the battery automatically to the discharge set-up after all the settings are implemented. The measurement is initiated and disconnects on completion. Fabrication

Table 1
Components and their magnitudes used for discharge unit

Resistors (all are 0.25 W, 1%, low TC, MFR, unless stated otherwise)
- R1 = 15 kΩ
- R2, R19 = 10 kΩ, 2 W, 10 turn potentiometer with dial unit
- R3, R4, R11, R12, R13, R15, R17 = 10 kΩ
- R5, R6 = 1 kΩ, 0.1% (10 kΩ if FS range = 100 μA)
- R7, R8, R9, R10 = 100 kΩ
- R14 = 2.2 kΩ
- R16 = 5.1 kΩ
- R18 = 39 kΩ

Capacitors
- C1, C3, C5 = 10 μf (electrolytic)
- C2, C4 = 0.1 μf (ceramic)

Semiconductors
- D1, D2 = diode 1N4148
- Tr1 = transistor BC 547B
- D3 = LM 336-2.5, 2.5 V band gap reference
- U1 = OP77, precision low offset, low drift quad Op-amp chip

Miscellaneous
- Piezo buzzer (intermittent type) 3–15 V
- DVM modules: 3.5 digit, 200 mV/2 V FS type
- d.c. power supply: dual ±5 V, 1 A

Table 2
Electrical properties of $((CH_3)_4N)_2Ag_{13}I_{15}$, silver boro-vanadate and silver boro-molybdate systems with sample code

Sample	Composition (F_1/F_2)	Sample code	$\sigma_{d.c.}$ ($\times 10^{-3}$ S cm^{-1})	$E_{d.c.}$ (eV)
$((CH_3)_4N)_2Ag_{13}I_{15}$	–	SITMAI	4.58	0.22 ± 0.02
60% AgI + 26.67% Ag_2O + 13.33% (F_1 B_2O_3 + F_2 V_2O_5)	0.5	SSBV-I	1.76	0.31 ± 0.01
	1.0	SSBV-II	0.57	0.38 ± 0.02
	2.0	SSBV-III	1.09	0.38 ± 0.03
60% AgI + 26.67% Ag_2O + 13.33% (F_1 B_2O_3 + F_2 MoO_3)	0.5	SSBM-I	1.34	0.35 ± 0.02
	1.0	SSBM-II	0.68	0.34 ± 0.01
	2.0	SSBM-III	0.57	0.31 ± 0.02

of the solid-state battery characterization of the battery with the new discharge unit are discussed in the next section.

3. Experimental

3.1. Preparation of $((CH_3)_4N)_2Ag_{13}I_{15}$

The polycrystalline sample $((CH_3)_4N)_2Ag_{13}I_{15}$ was prepared by mixing silver iodide and analar grade tetra-methyl ammonium iodide by a wet method. By contrast, the silver boro-vanadate system 60% AgI + 26.67% Ag_2O + 13.33% (F_1 B_2O_3 + F_2 V_2O_5) and silver boro-molybdate system 60% AgI + 26.67% Ag_2O + 13.33% (F_1 B_2O_3 + F_2 MoO_3) were prepared by melt quenching the molten liquid between stainless-steel plates in liquid nitrogen. Different compositions of the above systems, viz., F_1/F_2 = 0.5, 1.0, 2.0, were prepared from AR Grade Ag_2O, H_3BO_3, V_2O_5, MoO_3 with AgI prepared by precipitation. X-ray diffraction and differential scanning calorimetery studies confirmed the amorphous and glassy nature of the sample. The electrical properties of the above samples, such as d.c. conductivity at ambient temperature and activation energy below T_g, are given in Table 2 with sample codes.

3.2. Construction of solid-state batteries

Solid-state batteries with the following configuration were constructed at the laboratory level:

Ag|anode|solid electrolye|cathode|graphite|Ag

The batteries were fabricated with different cathode materials at various compositions and their performances were evaluated. As in our early investigation [5], the following types of cathode composition were used for the present battery characterization:

Component	Constituent	Weight ratio
Cathode I	I_2:C	9:1
Cathode II	I_2 + C:SE	2:1 with I_2:C = 9:1
Cathode III	I_2 + C + SE:TMAI	3:1 with I_2:C = 9:1

An anode–solid-electrolyte pellet of diameter 10 mm and thickness 1–3 mm was prepared by pressing a mixture of 0.08 g analar grade silver powder and 0.02 g finely powdered solid electrolyte into one disc and 0.25 g solid electrolyte as another disc, under a pressure of 2500 kg cm^{-2}. The cathode was made by pressing a 0.25 g mixture of cathode material such as iodine (I_2), graphite (C) and tetra methyl ammonium iodide (TMAI). The cells were constructed by sandwiching the anode|electrolyte|cathode pellets between the graphite disc and the silver electrode inside a Teflon container. The bottom and top faces of the container were each fitted with a silver electrode for external connections to the discharge unit. Immediately after cell fabrication, the open-circuit voltage (OCV) was measured with a high input impedance Philips Multi-meter, model 2525. The OCVs of the prepared solid-state batteries are listed in Table 3. It is observed that the distortion in OCV for the cathode I composition may be due to iodine activity with the solid electrolyte at the cathode interface.

The performance of each batteries was characterized by polarization and discharge studies. This involved connection of different loads across the test battery and monitoring of the terminal voltage of the battery and current flow through the load with high-performance meters. Formation of new compounds at the cathode|solid electrolyte interface increased the internal resistance of the battery and affected the discharge and polarization characteristics by altering the discharge current drain with discharge time. In the present work, a new discharge unit was designed and constructed so

Table 3
Open-circuit voltages of fabricated solid-state batteries

SSB material	I_2 + C (mV)	(I_2 + C): SE (mV)	(I_2 + C + SE): TMAI (mV)
SITMAI	558[a]	636	633
SSBV-I	652	670	662
SSBV-II	674	683	679
SSBV-III	683	681	676
SSBM-I	616[a]	684	673
SSBM-II	668	672	636
SSBM-III	669	686	654

[a] Distortion in open-circuit voltage due to iodine activity at cathode|sample interface.

that the current drawn from the test battery remains constant, irrespective of battery performance, with discharge time. Moreover, the new circuit does not require any external accessories such as variable load resistance and high-performance meters.

4. Results and discussion

The results of investigations of the polarization and discharge characteristics of the fabricated batteries using the new discharge unit are presented in this section. The OCVs obtained for the fabricated batteries by means of the conventional method are listed in Table 3. These values have been confirmed using the present discharge unit by setting the zero current; the OCVs are same as those listed within ±2 mV. The variation in battery potential is shown in Figs. 2–4 as a function of discharge current density for some of the fabricated batteries with different cathode compositions. The voltage was recorded 15 s after setting the discharge current.

In Fig. 2, the solid line and dots are polarization characteristics of the SITMAI-based battery with a conventional load resistor technique for different cathode compositions. The symbols are the polarization characteristics of the samples with the present discharge unit. It is clear that the polarization measurement with the present discharge unit indicate better performance over the conventional load resistor techniques. For a battery based on SITMAI and cathode I, the cathode pellets are highly reactive with solid electrolyte due to the presence of iodine and it is difficult to obtain polarization data from this battery.

To examine discharge characteristics, solid-state batteries with different cathode configuration were constructed and discharged at ambient temperature under constant current density using the present discharge circuit. Discharge was terminated when the battery potential reached 200 mV. The discharge curves for some of the samples are shown in Figs. 5–8.

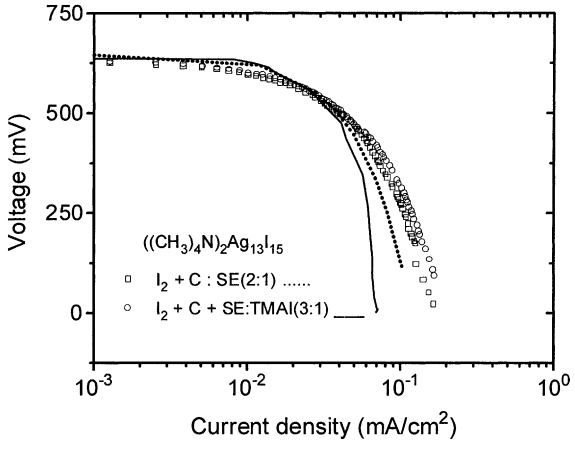

Fig. 2. Polarization curves for sample SITMAI with cathode II and cathode III compositions. Symbols correspond to results obtained from new discharge unit. Line and dots correspond to conventional load technique.

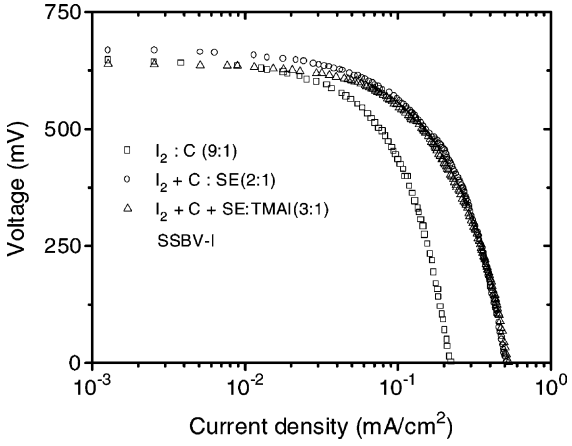

Fig. 3. Polarization curves for sample SSBV-I with different cathode compositions.

Discharge curves for the battery using SITMAI with cathode II and III configurations at a discharge rate of 50 μA are shown in Fig. 5. The addition of TMAI to the cathode composition improves the battery performance over a longer discharge time for the same discharge current. The initial rapid drop in the voltage is due to ohmic polarization and is followed by a gradual decrease in voltage due to discharge.

The discharge characteristics of the battery with SSBM III as solid electrolyte at three different cathode compositions are presented in Fig. 6. The discharge characteristics are highly dependent on the cathode composition. The addition of solid electrolyte to the cathode reduces the iodine activity at the cathode|solid electrolyte interface and displays better performance than the cathode I configuration. Further, the

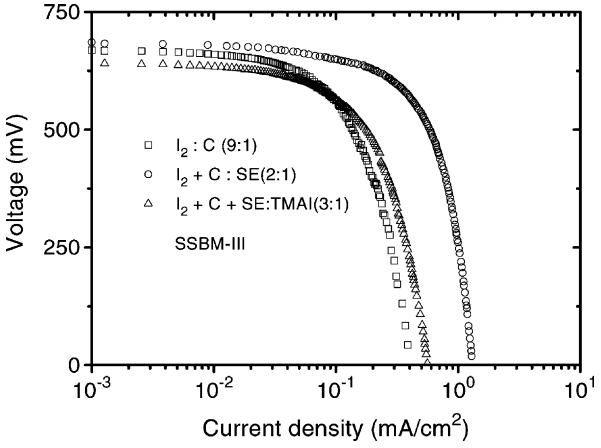

Fig. 4. Polarization curves for sample SSBM-III with different cathode compositions.

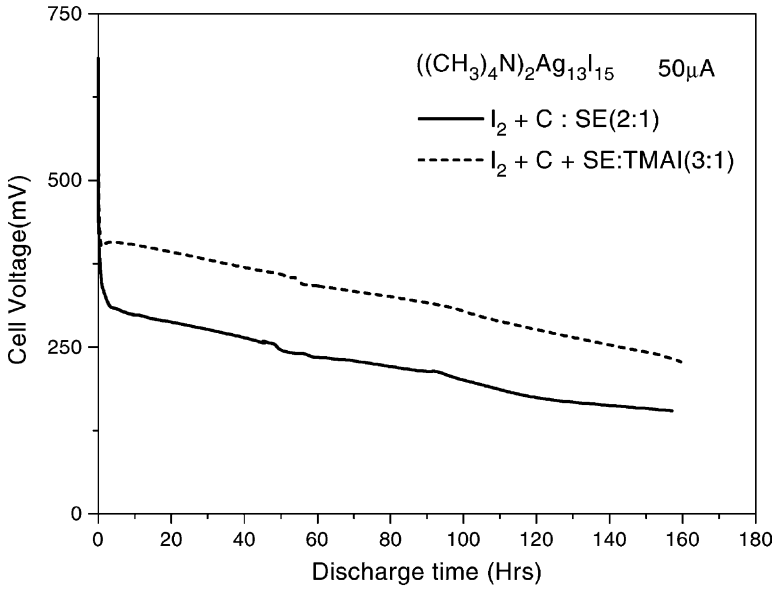

Fig. 5. Discharge characteristic curves for SITMAI with different cathode compositions at 50 μA current drain.

addition of the TMAI increases battery discharge due to the formation of a complex with the solid electrolyte, which reduces the sudden reaction of iodine with the electrolyte.

The discharge characteristics of the battery constructed with SSBV-II electrolyte and cathode II composition at different current drains (50–150 μA) are shown in Fig. 7. The discharge is the same for all drains during the initial period due to ohmic polarization. Thereafter, the discharge efficiency of the battery depends on the magnitude of the current drain. Similarly, Fig. 8 shows the effect of current drain on the discharge characteristics with a SSBV-I electrolyte and a cathode III composition.

During the discharge process, silver-ions are released from the anode and migrate to the cathode through the electrolyte to form AgI at the cathode|electrolyte interface. As battery discharge occurs continuously, the amount of discharge product AgI at the cathode interface increases and, hence, the internal resistance of the battery increases. Addition of solid electrolyte to the cathode material (cathode II) reduces the resistance of the charge-transfer at the sample|cathode interface and further addition of TMAI to the cathode material (cathode III) reduces the iodine activity at the cathode|sample interface by forming a conducting, inorganic, charge-transfer complex at the interface [21–26].

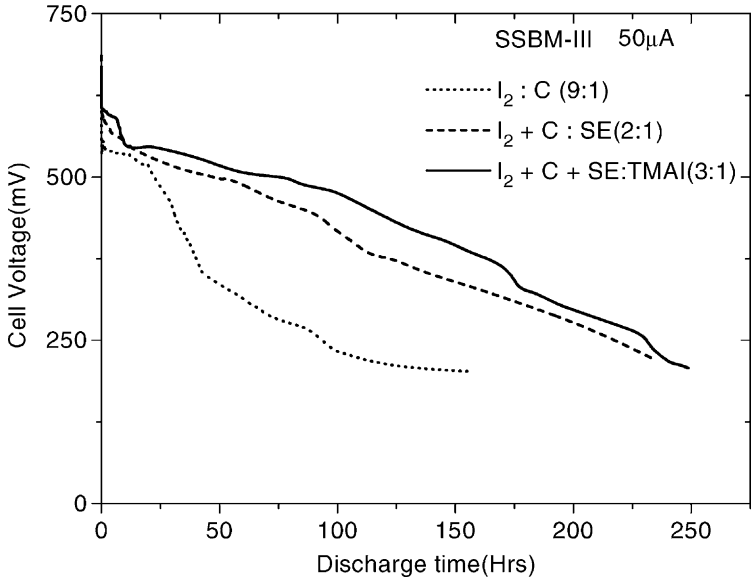

Fig. 6. Discharge characteristic curves for SSBM-III with different cathode compositions at 50 μA current drain.

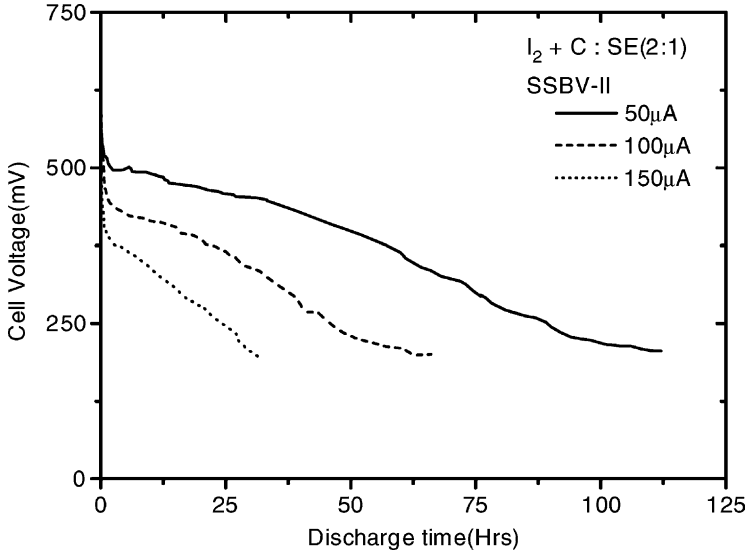

Fig. 7. Discharge characteristic curves for SSBV-II with cathode II composition at different current drains.

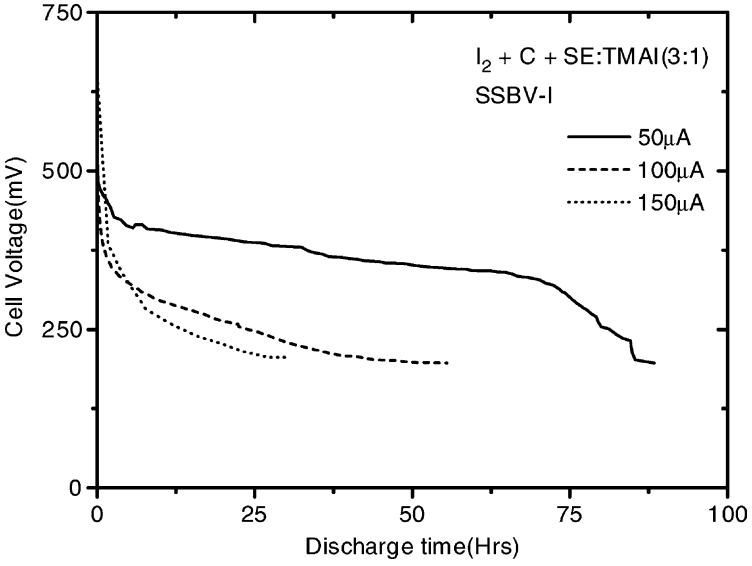

Fig. 8. Discharge characteristic curves for SSBV-I with cathode III composition at different current drains.

5. Conclusions

A new battery discharge unit has been constructed and is used to evaluate battery performance on polycrystalline and glassy solid electrolytes of silver-ion conducting solid-state materials. The new discharge unit does not require any other high input impedance devices, such as mV or μA meters, for battery characterization. The present study with the new discharge unit reveals that battery performance is very sensitive to the cathode composition. The addition of TMAI to the cathode material improves both the performance and stability of the solid-state batteries. The present discharge unit is being modified to examine both the charging and the discharging characteristics of solid-state batteries.

Acknowledgements

This work received financial assistance from the UGC research award scheme 30-64/98/SA-II and AICTE Project 8019/RDII/MOD/MAT/(95). One of author (R.M.) is grateful to UGC, Govt. of India, for financial assistance.

References

[1] B.V.R. Chowdari, S. Radhakrishna (Eds.), Materials for Solid State Batteries, World Scientific, Singapore, 1986.
[2] B.V.R. Chowdari, S. Radhakrishna (Eds.), Solid State Ionic Devices, World Scientific, Singapore, 1988.

[3] C.A.C. Sequeria, A. Hopper (Eds.), Solid State Batteries, NATO Advanced Study Institute Series, Martinus Nijhoff Publishers, Dordrecht, 1985.
[4] B.B. Scholtens, W. Van Gool, in: P. Hagenmuller, W. VanGool (Eds.), Solid Electrolytes, Academic Press, New York, 1978.
[5] N. Baskaran, G. Govindaraj, A. Narayanasamy, J. Power Sources 55 (1995) 153.
[6] C. Julien, Mater. Sci. Eng. B 6 (1990) 9.
[7] I.W. Mansen, J. Phys. Chem. 60 (1956) 806.
[8] A. Schiraldi, G. Chiodelli, A. Magistris, J. Appl. Electrochem. 6 (1976) 251.
[9] C.A. Vincent, Prog. Solid State Chem. 17 (1987) 145.
[10] J.R. Akridge, M. Balkanski (Eds.), Solid State Microbatteries, Plenum Press, New York, 1990.
[11] A. Sator, Compt. Rend. 34 (1952) 2283.
[12] K. Lehovec, J. Border, J. Electrochem. Soc. 101 (1954) 208.
[13] W.J. Vander Grienten, J. Electrochem. Soc. 103 (1956) 201.
[14] M. Ribbes, V. Derold, in: B.V.R. Chowdari, S. Radhakrishna (Eds.), Solid State Ionic Devices, World Scientific, Singapore, 1988.
[15] A. Levasseur, P. Vinatier, in: B.V.R. Chowdari, et al. (Eds.), Solid State Ionics: Science & Technology, World Scientific, Singapore, 1998, p. 421.
[16] J.B. Bates, H.J. Dudney, G.R. Gruzalski, R.A. Zhur, A. Choudhury, C.F. Luck, J. Power Sources 43/44 (1993) 103.
[17] J.D. Robertson, J. Power Sources 43/44 (1993) 103.
[18] A. Levasseur, M. Menetrier, R. Dormoy, G. Meunier, Mater. Sci. Eng. B3 (1989) 5.
[19] S.D. Jones, J.R. Akridge, J. Power Sources 43/44 (1993) 505.
[20] B.B. Owens, G.R. Argue, Science 157 (1967) 308.
[21] J.N. Brandely, P.D. Greene, Trans. Faraday Soc. 63 (1967) 424.
[22] B. Scrosati, F. Papaleo, G. Pistoia, J. Electrochem. Soc. 122 (1975) 339.
[23] T. Takahashi, S. Ikeda, O. Yamamoto, J. Electrochem. Soc. 117 (1970) 1.
[24] T. Takahashi, S. Ikeda, O. Yamamoto, J. Electrochem. Soc. 119 (1972) 477.
[25] G. Chiodelli, A. Magistris, A. Schraldi, Electrochim. Acta 19 (1974) 655.
[26] S. Geller, M.D. Lind, J. Chem. Phys. 52 (1970) 5854.